Distributed Computation for Sparse Recovery via Continuous-Time Neurodynamic Approach

You Zhao, Xiaofeng Liao[®], Fellow, IEEE, Mingliang Zhou[®], and Xing He[®], Member, IEEE

Abstract—Sparsity has been extensively employed in multimedia sensing and computing in consumer electronics, signal and image processing, depth video codec, adaptive sparse-type equalizer, blind speech separation, and machine learning. Throughout this paper, we propose a novel distributed projection neurodynamic approach for solving the Basis Pursuit (BP) with flexible partition methods in a distributed manner. The proposed neurodynamic approach requires only that the network is undirected and connected, and no node can access the entire matrix simultaneously. First, we equivalently formulate the BP into a standard distributed optimization problem with a flexible partition-by-blocks method to obtain global information, and discuss the equivalence of their optimality conditions. Then, we propose a distributed continuous-time neurodynamic approach on the basis of primal-dual dynamical systems and projection operators, and also study its global convergence property. Finally, numerical experiments on sparse signals and image recovery further verify the effectiveness and superiority of our proposed neurodynamic approach.

Index Terms—Distributed computation, neurodynamic approach, sparse recovery, continuous-time, global convergence.

I. INTRODUCTION

I N MANY real-world scientific and technical problems, such as signal and image processing for mass consumer electronics (TVs, VCRs, VCRs, camcorders, radios, portable digital cameras, and cameras on cell phones), and single-pixel camera imaging, one is faced with the task of inferring quantities of interest from measurement information. When the information acquisition process is linear, the problem is reduced to solving inverse problem of a linear system of equations. Mathematically, the observed data $b \in \mathbb{R}^m$ is connected to the signal of interest $x \in \mathbb{R}^n$ in the form: b = Ax, where m, denotes the amount of data measured. Actually, according

Manuscript received 12 January 2023; revised 3 March 2023; accepted 18 May 2023. Date of publication 2 June 2023; date of current version 26 April 2024. This work was supported in part by the National Key Research and Development Program of China under Grant 2018AAA0100101; in part by the National Natural Science Foundation of China under Grant 61932006 and Grant 62176027; and in part by the Fundamental Research Funds for the Central Universities under Project XDJK2020TY003. (Corresponding author: Xiaofeng Liao.)

You Zhao and Xing He are with the Chongqing Key Laboratory of Nonlinear Circuits and Intelligent Information Processing, School of Electronics and Information Engineering, Southwest University, Chongqing 400715, China (e-mail: Zhaoyou1991sdtz@163.com; hexingdoc@swu.edu.cn).

Xiaofeng Liao and Mingliang Zhou are with the College of Computer Science, Chongqing University, Chongqing 400044, China (e-mail: xfliao@cqu.edu.cn; mingliangzhou@cqu.edu.cn).

Digital Object Identifier 10.1109/TCE.2023.3281887

to linear algebra theory, when m < n, the linear observation b = Ax is underdetermined and there are infinitely many solutions. In other words, without additional information, it is impossible to recover a unique x from b for m < n. This fact is also related to Shannon's sampling theorem, which states that the sampling rate of a continuous-time signal must be twice its highest frequency to ensure reconstruction. It is surprising that a unique x can be reconstructed exactly in the case m < n when the signal has certain properties, and even more surprising that efficient algorithms do exist for reconstruction. The basic assumption that makes all this possible is sparsity (compressed sensing theory). Sparse representation has attracted the interest of many researchers and has a good reputation not only for theoretical research, but also for practical applications, including but not limited to adaptive sparse-type equalizer [1], [2], blind speech separation [3], multichannel DRM30 receiver [4], low complexity depth video codec [5], computer vision [6], signal processing and image processing [7] and compressed sensing [8] (see [9] for more applications). Mathematically, the sparse reconstruction can be expressed as an optimization problem:

$$\min \|x\|_0$$
, s.t. $Ax = b$, (1)

where the optimization variable $x \in \mathbb{R}^n$, $\|\cdot\|_0$ is the L_0 -(pseudo) norm of vector x, and $A \in \mathbb{R}^{m \times n}$ is measurement matrix with $m \ll n$. The problem (1) is a nonconvex problem owing to the L_0 -norm, which is NP-hard [10]. A popular approach is to replace L_0 -norm with the convex L_1 -norm (i.e., $\|x\|_1 = |x_1| + \cdots + |x_n|$), which can provide a satisfactory sparse solution under certain conditions [11]. Therefore, the original problem (1) can be convexly relaxed into the following convex optimization problem [12]:

$$\min \|x\|_1, \text{ s.t. } Ax = b,$$
 (2)

which is called Basis Pursuit (BP). In particular, the BP has a key role in sparse recovery. There are many classical centralized discrete-time algorithms proposed to solve the BP (2), which contain the matching pursuit (MP) algorithm [13] and its variants orthogonal MP (OMP) algorithm [14], alternating method of multiplier method (ADMM) [15], Lagrange dual method [16], gradient projection method [17], etc. In addition, when the observation vector *b* is interrupted by noises, there exist several strategies to address the variations of BP to obtain sparse signals, namely, Lasso [18].

Neurodynamic approaches for sparse recovery in science and engineering [19], [20], [21], [22], [23] have gained a wide interest due to the following advantages: their dynamical

behavior can be analyzed productively on the basis of the stability of the system and optimization theories, the global convergence and optimality of the neurodynamic approaches can be guaranteed; they can be implemented in hardware circuits and their parallel structure can eliminate the effects of high dimensionality and large density; in addition, using different discrete schemes, they can give rise to different discrete algorithms. For example, Balavoine et al. [19] proposed dynamical approach based on locally competitive algorithm (LCA) to solve Lasso problem to recovery sparse signals. Based on projection neural networks, Liu and Wang [20] presented several projection neurodynamic approaches in continuous-time to deal with BP (2) for reconstructing sparse signals. In [21], Feng et al. proposed a LPNN-LCA to tackle BP by incorporating Lagrange programming neural network (LPNN) with LCA. In addition, to obtain a faster convergence rate for sparse recovery, a dynamical approach with finite-time convergence for Lasso [22] and a projection neurodynamic approach with fixed-time convergence for BP [23] are investigated by using sliding mode technique. However, the proposed approaches (discretetime [14], [15], [16], [17], [18] and continuous-time [19], [20], [21], [22], [23]) just are centralized, i.e., they require a center to collect and process global information of (A, x)in BP (2).

In recent years, advances in data collection techniques have enabled a rapid scaling of the amount of data available in data science. Sparse optimizations in many modern applications concern very large-scale data such that they are no longer possible to deal with them on a single workstation running single-threaded code. Processing on a single workstation runs single-threaded code. It naturally becomes a viable option to migrate to a distributed method. Several approaches have been proposed to address general optimization problems, including BP and Lasso in a distributed manner. Gharesifard and Cortés [24] proposed a distributed differential inclusion (i.e., subgradient) approach to solve distributed nonsmooth convex problems. Liu and Wang [25] proposed a second-order neurodynamic approach for solving distributed nonsmooth constrained convex problems with the help of differential inclusion technique. Zhao et al. [26], [27] attempted to design distributed continuous-time neurodynamic approaches and their corresponding distributed discrete-time neurodynamic approaches for solving BP under row partition and column partition cases of matrix A, respectively. Later, Xu et al. [28] proposed a two-layer distributed projection neurodynamic approach for BP with row partition of matrix A.

It is worth noting that the distributed strategies mentioned above are either investigated only for row partition of matrix *A* or only for column partition of matrix *A*. However, there are very few researches on distributed algorithms or frameworks that can deal with BP with row partition and column partition of matrix *A* simultaneously. In our opinion, there are two difficulties in studying this problem, i.e., the first issue concerns how to equivalently convert BP into a standard distributed optimization problem; the second one is how to design

valid distributed neurodynamic approaches in a distributed manner that can simultaneously deal with non-smooth objective functions, primal and dual variables consensus constraints in the obtained distributed version of BP.

In this paper, we are motivated to study BP with block partition of matrix A (a general version of the row and column partition of matrix A) and propose a distributed continuous-time neurodynamic approach, and analyze its optimality and convergence properties. The summary of the main contributions is as follows:

- Based on distributed consensus theorem, we reformulate the original BP (2) in a standard distributed optimization problem with flexible block partition of matrix A, which is a generalization for the partition by rows and columns of matrix A [26], [27], [28]. Specifically, for the issue caused by the row partition of the matrix A, an equivalent transformation is performed by using an optimization variable consensus constraint, and for the challenge caused by column partition of matrix A, we introduce a supplementary variable to equivalently decouple the original linear observation constraint into a standard distributed version. It implies that the distributed approaches [26], [27], [28] mentioned above can not be used directly to solve the standard distributed optimization problem obtained by general block partition of the matrix A.
- By combining derivative feedback technique of optimization variable and the projection operators, a novel distributed continuous-time projection neurodynamic approach (DCPNA-B) is proposed, where the projection operators are used to avoid the differential inclusion (subgradient calculation of L_1 -norm) method [24], [25] to eliminate the difficulty of choosing an appropriate subgradient at a non-differential point (see Fig. 3); moreover, the primal-dual dynamics is employed to cope with the consensus constraints and the modified linear observation constraint, which avoids the inverse operation of $(AA^T)^{-1}$ [28], which can reduce the computational complexity of image and signal reconstruction in consumer electronics.
- Two novel Lyapunov functions for rigorously proving the global convergence of DCPNA-B are presented. Because the projection operators are employed in DCPNA-B instead of the differential inclusion (subgradient) and soft-threshold methods, where the Lyapunov analysis tools in [24], [25], [26], [27], [28] are not applicable.

The paper is organized as follows. Some essential notations and preliminaries are presented in Section II. The Basis Pursuit (BP) is reformulated in a distributed optimization problem with block partition of matrix A, which is presented in Section III. In Section IV, a distributed continuous-time projection neurodynamic approach (DCPNA-B) is proposed to solve distributed version of BP, and the convergence and optimality of DCPNA-B is also discussed. In Section V, numerical experiments on sparse recovery are performed to demonstrate the effectiveness and superiority of our proposed DCPNA-B. Finally, a brief conclusion is given in Section VI.

II. Preliminaries

A. Notations

Let \mathbb{R} , \mathbb{R}^{np} be the sets of real numbers, np-dimensional column vectors, respectively. The superscript T means transpose. Let $|\cdot|$ be the absolute value. $||x|| = \left(\sum_{i=1}^n x_i^2\right)^{\frac{1}{2}}$ is the Euclidean norm, $||x||_1 = \sum_{i=1}^n |x_i|$ represents the L_1 -norm and $||x||_0$ is the 0-norm which calculates the number of non-zero elements. $I_n \in \mathbb{R}^{n \times n}$ is an identity matrix. The \otimes is the Kronecker product. The $\delta_{\max}(A)$ means the maximum singular value of matrix $A \in \mathbb{R}^{m \times n}$. For matrix $L \in \mathbb{R}^{n \times n}$, denote $||x||_L^2 = x^T L x$. For any $x \in \mathbb{R}^n$, the \dot{x} (the rate of change of neuronal state of neuron x) represents the derivative of variable x (the state of neuron x) with respect to t, i.e., $\dot{\mathbf{x}} = \frac{d\mathbf{x}}{dt} = \left(\frac{d\mathbf{x}_1}{dt}, \dots, \frac{d\mathbf{x}_n}{dt}\right)^T \in \mathbb{R}^n.$

B. Subdifferential

Definition 1: The function $\varphi : \mathbb{R}^{np} \to \mathbb{R}$ is generally convex (possible non-smooth) if the following condition holds

$$\varphi(w) \ge \varphi(u) + \eta^T(w - u), \ \forall u \in \mathbb{R}^{np},$$
 (3)

where $\eta \in \partial \varphi(w)$, η is the subgradient of φ at w.

Moreover, $\partial \varphi(w)$ is subdifferential of φ at w, which is given by

$$\partial \varphi(w) = \left\{ \eta | \varphi(u) - \varphi(w) \right. \\ \geq \eta^{T}(u - w), \ \forall u \in \mathbb{R}^{np} \right\}. \tag{4}$$

C. Projection Operator

Definition 2: Let Ω be a closed and convex set, then the projection operator is

$$P_{\Omega}(u) = arg\min_{w \in \Omega} ||u - w||.$$

If $\Omega = [-1, 1]^{np} = \{u \in \mathbb{R}^{np} | -1 \le u_i \le 1, i = 1, \dots, np\},\$ then, for any i, the projection operator $P_{[-1,1]^{np}}(u_i)$ (see the middle subfigure in Fig. 3) is

$$P_{[-1,1]^{np}}(u_i) = \begin{cases} 1, & \text{if } u_i > 1, \\ u_i, & \text{if } -1 \le u_i \le 1, \\ -1, & \text{if } u_i < -1, \end{cases}$$

i.e.,

$$P_{[-1,1]^{np}}(u_i) = \min\{\max\{u_i, -1\}, 1\}.$$

Lemma 1 [20]: For projection operator, the following properties hold

$$(u - P_{\Omega}(u))^{T} (P_{\Omega}(u) - w) \ge 0, \forall u \in \mathbb{R}^{np}, w \in \Omega, (5a)$$

$$\|w - u\|^{2} \ge (w - u)^{T} (P_{\Omega}(w) - P_{\Omega}(u))$$

$$\ge \|P_{\Omega}(u) - P_{\Omega}(w)\|^{2}, \forall w, u \in \mathbb{R}^{np}, \qquad (5b)$$

$$u = P_{[-1,1]^{np}}(u + w)$$

$$\Rightarrow (\zeta - u)^{T} (-w) \ge 0, \forall \zeta \in [-1, 1]^{np}. \qquad (5c)$$

Lemma 2 [26]: The Bregman divergence of h at w and uis given by $D_h(w, u) = h(w) - h(u) - (w - u)^T \nabla h(v)$. Let $h(w) = \frac{1}{2} ||w||^2 - \frac{1}{2} ||w - P_{\Omega}(w)||^2$, one has 1): $\nabla_{w}^{z}h(w) = \tilde{P}_{\Omega}(w)$.

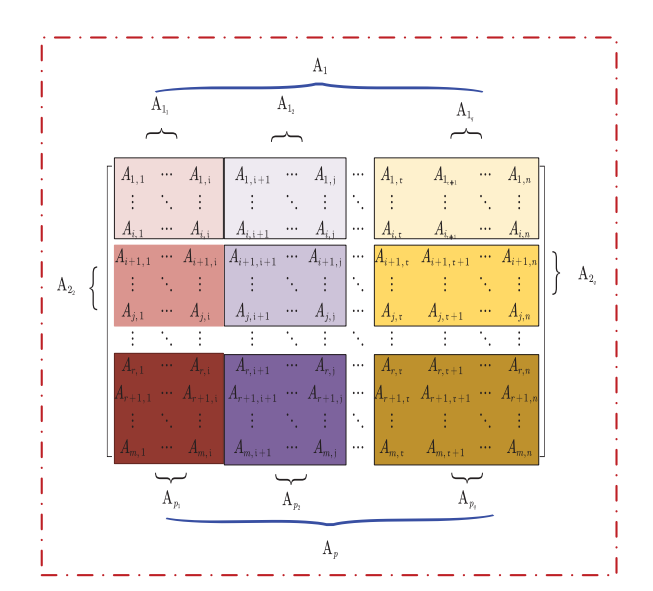


Fig. 1. The block of A with $0 , <math>0 < q \le m$, and $p, q \in \mathbb{R}$.

2): $D_h(w, u)$ is continuous and differentiable with respect to w. Moreover, $D_h(w, v) \ge \frac{1}{2} \|P_{\Omega}(w) - P_{\Omega}(v)\|^2$ implies that function h is convex.

D. Graph Theory

Define an undirected graph as $\mathcal{G} = (\mathcal{V}, \mathcal{E}, \mathcal{A})$, where $\mathcal{V} =$ (ν_1,\ldots,ν_n) is a set of vertexes or agents, $\mathcal{E}\subseteq\mathcal{V}\times\mathcal{V}$ being a set of edges, $A = \{a_{ij}\} \in \mathbb{R}^{n \times n}$ is a weighted adjacency matrix of G with $a_{ij} > 0$ if agent i and agent j are connected, otherwise $a_{ii} = 0$. When there is a path between any pair of distinct vertex/agnet i and vertex/agnet j, the graph \mathcal{G} is called connected. Correspondingly, the Laplacian matrix of \mathcal{G} is $L_n =$ $(l_{ij})_{n\times n}=D-\mathcal{A}$, where $D=\operatorname{diag}\{d_1,d_2,\ldots,d_n\}\in\mathbb{R}^{n\times n}$, and $d(v_i) = \sum_{j=1}^n a_{ij}$ is the degree of vertex v_i . Moreover, the Laplacian matrix L_n is semi-positive definite with a simple eigenvalue 0, i.e., $L_n 1_n = 0_n$.

III. DISTRIBUTED BASIS PURSUIT (BP) PROBLEM BASED ON BLOCK PARTITION OF MATRIX A

In this section, we show how to equivalently transformed the original BP (2) into a standard distributed optimization problem with block partition of matrix A.

We segment the matrix A by block according to the format in Fig. 1 as follows:

where each block $A_{ij} \in \mathbb{R}^{m_i \times n_j}$, $i = 1, \ldots, p$; $j = 1, \ldots, q$, $\sum_{i=1}^p m_i = m$ and $\sum_{j=1}^q n_i = n$. The variable $b \in \mathbb{R}^m$ is correspondingly decomposed into $(b_1^T, \ldots, b_p^T)^T \in \mathbb{R}^m$.

Assumption 1: The matrix $A_{ij} \in \mathbb{R}^{m \times n}$ has row-full rank

and satisfies $m \ll n$.

Assumption 2: The communication graph $\mathcal{G}_i^{\text{row}}$, $\mathcal{G}_i^{\text{col}}$ with any fixed i = 1, ..., p; j = 1, ..., q are undirected and connected.

Every node i_i only computes its local variable $x_{i_i} \in \mathbb{R}^{n_j}$, and they combine states of nodes $i_j, j = 1, ..., q$ variables forming $\mathbf{x}_i = \left[\mathbf{x}_{i_1}^T, \dots, \mathbf{x}_{i_q}^T\right]^T \in \mathbb{R}^n$. Moreover, all $\mathbf{x}_i, i = 1, \dots, p$ need to be consensus, i.e., $\mathbf{x}_i = \mathbf{x}_l, i, l = 1, \dots, p$ or $\mathbf{x}_{li} = \mathbf{x}_{li}, i, l = 1, \dots, p; j = 1, \dots, q$. In addition, according

to the block partition property of matrix A in Fig. 1, Ax = b in BP (2) is formulated as

$$\begin{bmatrix} \sum_{j=1}^{q} \mathbf{A}_{1j} \mathbf{x}_{1j} \\ \vdots \\ \sum_{j=1}^{q} \mathbf{A}_{pj} \mathbf{x}_{pj} \end{bmatrix} = \begin{bmatrix} b_1 \\ \vdots \\ b_p \end{bmatrix} = b \in \mathbb{R}^m.$$
 (6)

Thus, the original BP (2) can be equivalently transformed into

$$\min_{\mathbf{x}} \sum_{i=1}^{p} \sum_{j=1}^{q} \|\mathbf{x}_{i_{j}}\|_{1}$$
s.t.
$$\sum_{j=1}^{q} \mathbf{A}_{i_{j}} \mathbf{x}_{i_{j}} = b_{i},$$

$$\mathbf{x}_{i_{j}} = \mathbf{x}_{l_{j}}, \forall i, l = 1, \dots, p; j = 1, \dots, q.$$
(7)

Note that the consensus constraints $x_{i_j} = x_{l_j}, \forall i, l = 1, ..., p, j = 1, ..., q$ in (7) can be converted to

$$\sum_{l=1}^{p} \mathfrak{b}_{il}^{j} (\mathbf{x}_{ij} - \mathbf{x}_{lj}) = 0_{n_j}, i = 1, \dots, p; j = 1, \dots, q,$$
 (8)

by using the property of Laplace matrix property of L^{col} .

It is worth noting that the equality constraint (6) is globally coupled, in order to obtain the standard distributed optimization problem of BP (2), the decoupling method for the coupled constraints (6) is as follows:

For any fixed $i=1,\ldots,p$, we can decompose the variable b_i into $b_i=\sum_{j=1}^q b_{i_j}\in\mathbb{R}^{m_i}$ with $b_{i_j}=\frac{1}{q}b_i\in\mathbb{R}^{m_i}$. Introducing a supplementary variable $y\in\mathbb{R}^{mq}$ and using the property of Laplace matrix property of \mathcal{L}^{row} , the equations $\sum_{j=1}^q A_{i_j}x_{i_j}=b_i, i=1,\ldots,p; j=1,\ldots,q$ in (7) (i.e., Eq. (6)) is equivalently decoupled into the following distributed form

$$\begin{bmatrix} A_{1_{1}}x_{1_{1}} - b_{1_{1}} + \sum_{k=1}^{q} \mathfrak{a}_{1v}^{1}(y_{1_{1}} - y_{1_{v}}) = 0_{m_{1}} \\ \vdots \\ A_{1_{q}}x_{1_{q}} - b_{1_{q}} + \sum_{k=1}^{q} \mathfrak{a}_{qv}^{1}(y_{1_{q}} - y_{1_{v}}) = 0_{m_{1}} \\ \vdots \\ A_{p_{1}}x_{p_{1}} - b_{p_{1}} + \sum_{k=1}^{q} \mathfrak{a}_{1v}^{p}(y_{p_{1}} - y_{p_{v}}) = 0_{m_{p}} \\ \vdots \\ A_{p_{q}}x_{p_{q}} - b_{p_{q}} + \sum_{k=1}^{q} \mathfrak{a}_{qv}^{p}(y_{p_{q}} - y_{p_{v}}) = 0_{m_{p}} \end{bmatrix} \in \mathbb{R}^{mq}. (9)$$

Combining with (7), (8) and (9), the BP (2) can be equivalently transformed as a standard distributed optimization problem

$$\min_{\mathbf{x},\mathbf{y}} \sum_{i=1}^{p} \sum_{j=1}^{q} \|\mathbf{x}_{i_{j}}\|_{1}
\text{s.t.} \quad \mathbf{A}_{i_{j}} \mathbf{x}_{i_{j}} - b_{i_{j}} + \sum_{\nu=1}^{q} \mathfrak{a}_{j\nu}^{i} (\mathbf{y}_{i_{j}} - \mathbf{y}_{i_{\nu}}) = \mathbf{0}_{m_{i}},
\sum_{l=1}^{p} \mathfrak{b}_{il}^{j} (\mathbf{x}_{i_{j}} - \mathbf{x}_{l_{j}}) = \mathbf{0}_{n_{j}}, i = 1, \dots, p; j = 1, \dots, q, \quad (10)$$

and the compact form of the distributed problem (10) is

$$\min_{\substack{x,y \\ s.t.}} \|x\|_{1}
s.t. \quad Ax - b - L_{c}y = 0_{mq},
L_{r}x = 0_{mp},$$
(11)

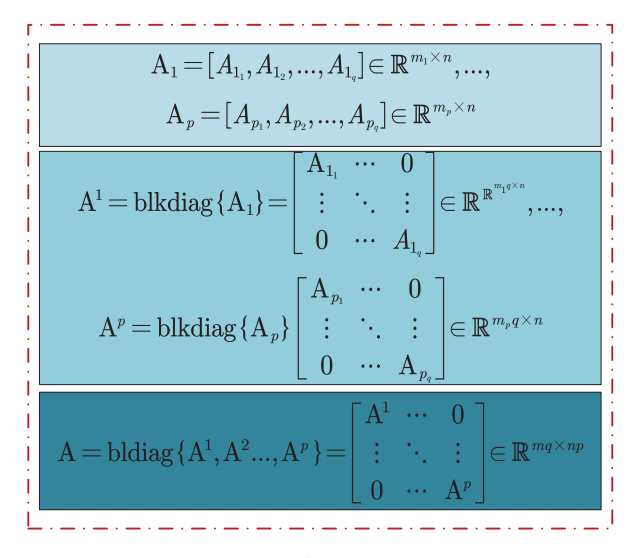


Fig. 2. The matrices of A_1 , A_p , A^1 , A^p and A.

where $\mathbf{x} = \begin{bmatrix} \mathbf{x}_{1_1}, \dots, \mathbf{x}_{1_q}, \dots, \mathbf{x}_{p_1}, \dots, \mathbf{x}_{p_q} \end{bmatrix} \in \mathbb{R}^{np},$ $\mathbf{y} \in \mathbb{R}^{mq}, \ L_c = \text{blkdiag} \ \{L^{\operatorname{col}} \otimes I_{m_1}, \dots, L^{\operatorname{col}} \otimes I_{m_p}\} \in \mathbb{R}^{mq \times mq}, \ L_r = L^{\operatorname{row}} \otimes I_n \in \mathbb{R}^{np \times np}.$ Moreover, $\mathbf{A} = \text{bldiag} \ \{\mathbf{A}^1, \mathbf{A}^2, \dots, \mathbf{A}^p\} \in \mathbb{R}^{mq \times np}$ is a block diagonal matrix, where $\mathbf{A}^1 = \text{blkdiag} \ \{\mathbf{A}_1\} \in \mathbb{R}^{m_1q \times n}, \dots, \mathbf{A}^p = \text{blkdiag} \ \{\mathbf{A}_p\} \in \mathbb{R}^{m_pq \times n} \text{ and } \mathbf{A}_1 = (A_{1_1}, A_{1_2}, \dots, A_{1_q}) \in \mathbb{R}^{m_1 \times n}, \dots, \mathbf{A}_p = \{A_{p_1}, A_{p_2}, \dots, A_{p_q}\} \in \mathbb{R}^{m_p \times n} \text{ with } \sum_{i=1}^p m_i = m, \text{ which are shown in Fig 2}.$

IV. DISTRIBUTED PROJECTION NEURODYNAMIC APPROACHES FOR PROBLEM (11)

In this section, distributed projection neurodynamic approach in continuous-time is proposed to deal with the problem (11) with block partition case of matrix A.

A. Distributed Continuous-Time Projection Neurodynamic Approach for Problem (11)

For any fixed i = 1, ..., p and j = 1, ..., q, we propose a distributed continuous-time projection neurodynamic approach (named as DCPNA-B) as follows:

$$\begin{cases}
\dot{x}_{ij} = -P_{[-1,1]^{n_j}}(x_{ij} + z_{ij}) - A_{i_j}^T \lambda_{i_j} \\
- \sum_{l=1}^p b_{il}^j (u_{i_j} - u_{l_j}), \\
\dot{z}_{i_j} = -\frac{1}{2} z_{i_j} + \frac{1}{2} P_{[-1,1]^{m_i}}(x_{i_j} + z_{i_j}), \\
\dot{y}_{i_j} = \sum_{\nu=1}^q a_{j\nu}^i (\lambda_{i_j} - \lambda_{i_\nu}), \\
\dot{\lambda}_{i_j} = A_{i_j}(x_{i_j} + \dot{x}_{i_j}) - b_{i_j} \\
- \sum_{\nu=1}^q a_{j\nu}^i (y_{i_j} + \lambda_{i_j} - y_{i_\nu} - \lambda_{i_\nu}), \\
\dot{u}_{i_j} = \sum_{l=1}^p b_{jl}^i (x_{i_j} + \dot{x}_{i_j} - x_{l_j} - \dot{x}_{l_j}),
\end{cases} (12)$$

correspondingly, the compact form of (12) is

$$\begin{cases} \dot{x} = -P_{[-1,1]^{np}}(x+z) - A^{T}\lambda - L_{r}u, \\ \dot{z} = -\frac{1}{2}z + \frac{1}{2}P_{[-1,1]^{np}}(x+z), \\ \dot{y} = L_{c}\lambda, \\ \dot{\lambda} = A(x+\dot{x}) - b - L_{c}(y+\lambda), \\ \dot{u} = L_{r}(x+\dot{x}), \end{cases}$$
(13)

Lemma 3: For any given initial values $(x_0, z_0, u_0, \lambda_0, y_0) \in \mathbb{R}^{np} \times [-1, 1]^{np} \times \mathbb{R}^{np} \times \mathbb{R}^{mq} \times \mathbb{R}^{mq}$, the DCPNA-B (13) has a unique solution.

Proof: Let $\mathbf{y}^1 = (\mathbf{x}^1, \mathbf{z}^1, \mathbf{u}^1, \lambda^1, \mathbf{y}^1)$ and $\mathbf{y}^2 = (\mathbf{x}^2, \mathbf{z}^2, \mathbf{u}^2, \lambda^2, \mathbf{y}^2) \in \mathbb{R}^{np} \times [-1, 1]^{np} \times \mathbb{R}^{np} \times \mathbb{R}^{mq} \times \mathbb{R}^{mq}$ be any two solutions of DCPNA-B (13) with the same initial value $\mathbf{y}_0 = (\mathbf{x}_0, \mathbf{z}_0, \mathbf{u}_0, \lambda_0, \mathbf{y}_0)$. If $\mathbf{y}^1 \neq \mathbf{y}^2$, then there exist $\tau > 0$ and $\varpi > 0$, such that $\mathbf{y}^1(t) \neq \mathbf{y}^2(t)$ with any $t \in [\tau, \tau + \varpi]$. Define

$$\mathcal{F}(y) = \begin{pmatrix} -P_{[-1,1]^{np}}(x+z) - A^T \lambda - L_r u \\ -\frac{1}{2}z + \frac{1}{2}P_{[-1,1]^{np}}(x+z) \\ L_c \lambda \\ A(x+\dot{x}) - b - L_c(y+\lambda) \\ L_r(x+\dot{x}) \end{pmatrix}.$$

Since $\mathcal{F}(\mathbf{y})$ is Lipschitz continuous on $t \in [0, \tau + \varpi]$, i.e., there exists a Lipschitz constant such that

$$\begin{split} & \left\| \mathcal{F} \left(\mathbf{y}^{1} \right) - \mathcal{F} \left(\mathbf{y}^{2} \right) \right\| \\ & \leq \left(\frac{5}{2} + \delta_{\max}(A) + \delta_{\max}(L_{r}) \right) \left\| \mathbf{z}^{2} - \mathbf{z}^{1} \right\| \\ & + \left(2 + 2\delta_{\max}(A) + 2\delta_{\max}(L_{r}) \right) \left\| \mathbf{x}^{2} - \mathbf{x}^{1} \right\| \\ & + \delta_{\max}(L_{c}) \left\| \mathbf{y}^{2} - \mathbf{y}^{1} \right\| + \left(\delta_{\max}(A) + 2\delta_{\max}(L_{c}) + \delta_{\max}(A)^{2} + \delta_{\max}(L_{r}) \delta_{\max}(A) \right) \left\| \lambda^{2} - \lambda^{1} \right\| \\ & + \left(\delta_{\max}(L_{r}) + \delta_{\max}(L_{r}) \delta_{\max}(A) \right) \left\| \mathbf{u}^{2} - \mathbf{u}^{1} \right\| \\ & \leq \left(\frac{9}{2} + \left(4 + \delta_{\max}(A) + 2\delta_{\max}(L_{r}) \right) \delta_{\max}(A) + 4\delta_{\max}(L_{r}) + 3\delta_{\max}(L_{c}) + \delta_{\max}(L_{r})^{2} \right) \left\| \mathbf{y}^{1} - \mathbf{y}^{2} \right\|, \end{split}$$

where $l = \left(\frac{9}{2} + (4 + \delta_{\max}(A) + 2\delta_{\max}(L_r))\delta_{\max}(A) + 4\delta_{\max}(L_r) + 3\delta_{\max}(L_c) + \delta_{\max}(L_r)^2\right)$ is a Lipschitz constant, which yields

$$\begin{aligned} &\frac{d}{dt} \frac{1}{2} \| \mathbf{y}^1(t) - \mathbf{y}^2(t) \|^2 \\ &= \left(\mathbf{y}^1(t) - \mathbf{y}^2(t) \right)^T \left(G\left(\mathbf{y}^1(t) \right) - G\left(\mathbf{y}^2(t) \right) \right) \\ &\leq \mathbb{I} \| \mathbf{y}^1(t) - \mathbf{y}^2(t) \|^2, \, \forall t \in [0, \tau + \varpi]. \end{aligned}$$

Integrating the above inequality from 0 to $\tau + \varpi$, it follows that $y_1 \neq y_2, \forall t \in [0, \tau + \varpi]$ with the same initial values $y_0 = (x_0, z_0, u_0, \lambda_0, y_0)$. This leads to a contradiction. Thus, the proof is thereby completed.

Theorem 1: Under **Assumptions** 1, 2, $(x^*, z^*, u^*, \lambda^*, y^*) \in \mathbb{R}^{np} \times [-1, 1]^{np} \times \mathbb{R}^{np} \times \mathbb{R}^{mq} \times \mathbb{R}^{mq}$ is an equilibrium of DCPNA-B (13) if and only if $x^* \in \mathbb{R}^{np}$ is an optimal solution of problem (11).

Proof:

(i) Necessity: if $x^* \in \mathbb{R}^{np}$ is an optimal solution of problem (11), according to the Karush-Kuhn-Tucker (KKT) conditions, there exist y^* , λ^* , such that

$$0_{np} \in \partial \|\mathbf{x}^*\|_1 + \mathbf{A}^T \lambda^* + L_r \mathbf{u}^*, \tag{14a}$$

$$0_{nn} = L_r \mathbf{x}^*, \tag{14b}$$

$$0_{mq} = Ax^* - b - L_c y^*, (14c)$$

$$0_{ma} = L_c \lambda^*. \tag{14d}$$

Let $z^* = \partial \|x^*\|_1 = (\partial |x^*_{1_{1_1}}|, \dots, \partial |x^*_{p_{q_{n_q}}}|)^T \in \mathbb{R}^{np}$ with $i = 1, \dots, p; j = 1, \dots, q; r = 1, \dots, n_j$ and it contains $\begin{cases} 1, & x^*_{i:} > 0, \end{cases}$

$$z_{i_{j_r}}^* = \partial \left| \mathbf{x}_{i_{j_r}}^* \right| = \begin{cases} 1, & \mathbf{x}_{i_{j_r}}^* > 0, \\ [-1, 1], \mathbf{x}_{i_{j_r}}^* = 0, \\ -1, & \mathbf{x}_{i_{j_r}}^* < 0, \end{cases}$$
(15)

The equation (15) is equivalent to (see Fig. 3)

$$z^* = P_{[-1,1]^{np}}(x^* + z^*) = \partial \|x^*\|_1.$$
 (16)

According to (16), the Eq. (14a) can be equivalently written as $0_{np} = P_{[-1,1]^{np}}(\mathbf{x}^* + \mathbf{z}^*) + \mathbf{A}^T \lambda^* + L_r \mathbf{u}^*$. It means that $(\mathbf{x}^*, \mathbf{z}^*, \mathbf{u}^*, \lambda^*, \mathbf{y}^*) \in \mathbb{R}^{np} \times [-1, 1]^{np} \times \mathbb{R}^{np} \times \mathbb{R}^{mq} \times \mathbb{R}^{mq}$ is an equilibrium of DCPNA-B (13).

(ii) Sufficiency: when $(x^*, z^*, u^*, \lambda^*, y^*)$ is an equilibrium of DCPNA-B (13), one has

$$0_{np} = -P_{[-1,1]^{np}}(\mathbf{x}^* + \mathbf{z}^*) - \mathbf{A}^T \lambda^* - L_r \mathbf{u}^*, \qquad (17a)$$

$$0_{np} = -z^* + P_{[-1,1]^{np}}(x^* + z^*), \tag{17b}$$

$$0_{np} = L_r x^*, (17c)$$

$$0_{mq} = Ax^* - b - L_c(y^* + \lambda^*), \tag{17d}$$

$$0_{ma} = L_c \lambda^*, \tag{17e}$$

where the Eq. (17d) becomes $0_{mq} = Ax^* - b - L_c y^*$ according to (17e), and the Eq. (17a) reduces to $0_{np} = P_{[-1,1]^{np}}(x^* + z^*) + A^T \lambda^* + L_r u^*$, which combines (17b) with (16) to obtain $0_{np} \in \partial ||x^*||_1 + A^T \lambda^* + L_r u^*$. To sum up, we can obtain that $x^* \in \mathbb{R}^{np}$ is an optimal solution of the problem (11).

Next, we will show the convergence results of the DCPNA-B (13). Let $(x^*, z^*, u^*, \lambda^*, y^*)$ be an equilibrium of DCPNA-B (13). Define a Lyapunov function as $V(x, z, y, \lambda, u) = V_0(x, z, y) + V_1(x) + V_2(z) + V_3(y) + V_4(\lambda) + V_5(u)$ with

$$V_{0}(\mathbf{x}, \mathbf{z}, \mathbf{y}) = h(\mathbf{x} + \mathbf{z}) - h(\mathbf{x}^{*} + \mathbf{z}^{*}) + (\mathbf{A}\mathbf{x} - \mathbf{b} - L_{c}\mathbf{y})^{T}\lambda^{*} - (\mathbf{z} - \mathbf{z}^{*})^{T}\mathbf{z}^{*} - (\mathbf{x} - \mathbf{x}^{*})^{T}L_{r}\mathbf{u}^{*},$$

$$V_{1}(\mathbf{x}) = \frac{1}{2}\|\mathbf{x} - \mathbf{x}^{*}\|^{2}, V_{2}(\mathbf{z}) = \frac{1}{2}\|\mathbf{z} - \mathbf{z}^{*}\|^{2},$$

$$V_{3}(\mathbf{y}) = \frac{1}{2}\|\mathbf{y} - \mathbf{y}^{*}\|^{2}, V_{4}(\lambda) = \frac{1}{2}\|\lambda - \lambda^{*}\|^{2},$$

$$V_{5}(\mathbf{u}) = \frac{1}{2}\|\mathbf{u} - \mathbf{u}^{*}\|^{2},$$
(18)

where $h(x + z) = -\frac{1}{2} \|x + z - P_{[-1,1]^{np}}(x + z)\|^2 + \frac{1}{2} \|x + z\|^2$. The function h is convex and differentiable of x and z, i.e., $\nabla_x h(x + z) = P_{[-1,1]^{np}}(x + z)$, $\nabla_z h(x + z) = P_{[-1,1]^{np}}(x + z)$ from **Lemma 2**.

By using the convexity of h(x+z) with respect to x and z, one has

$$\frac{1}{2} \|\mathbf{x} - \mathbf{x}^*\|^2 + \frac{1}{2} \|\mathbf{z} - \mathbf{z}^*\|^2 + h(\mathbf{x} + \mathbf{z}) - h(\mathbf{x}^* + \mathbf{z}^*)$$

$$\geq (\mathbf{x} - \mathbf{x}^*)^T \mathbf{z}^* + (\mathbf{z} - \mathbf{z}^*)^T \mathbf{z}^* + \frac{1}{2} \|\mathbf{x} - \mathbf{x}^*\|^2$$

$$+ \frac{1}{2} \|\mathbf{z} - \mathbf{z}^*\|^2 + (\mathbf{z} - \mathbf{z}^*)^T$$

$$\times (P_{[-1,1]^{np}}(\mathbf{x} + \mathbf{z}^*) - P_{[-1,1]^{np}}(\mathbf{x}^* + \mathbf{z}^*))$$

$$\geq (\mathbf{x} - \mathbf{x}^*)^T \mathbf{z}^* + (\mathbf{z} - \mathbf{z}^*)^T \mathbf{z}^*, \tag{19}$$

where the last inequality holds due to the Young inequality.

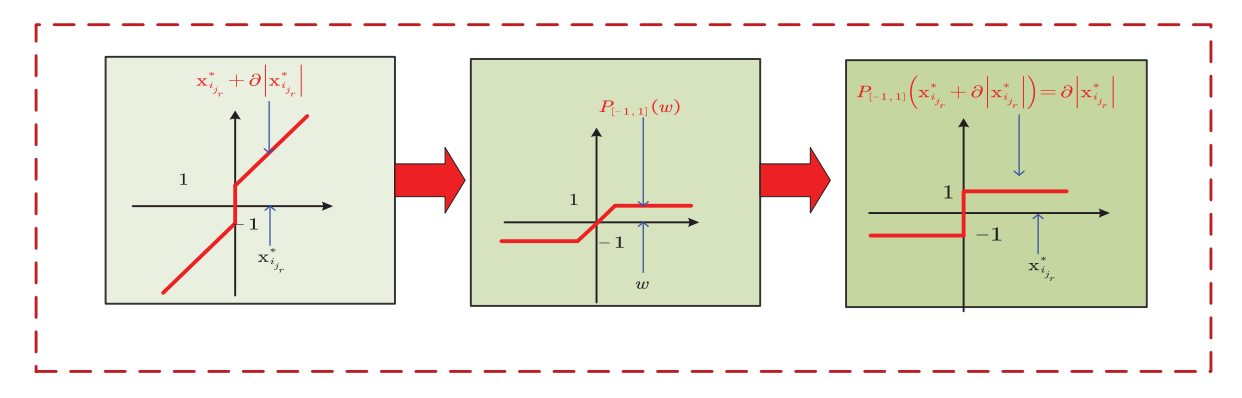


Fig. 3. The relationship between the projection operator $P_{[-1,1]}(\mathbf{x}_{i_{j_r}}^* + \partial |\mathbf{x}_{i_{j_r}}^*|)$ and subgradient $\partial |\mathbf{x}_{i_{j_r}}^*|$.

Theorem 2: Suppose **Assumptions** 1, 2 hold. For any $(x_0, z_0, u_0, \lambda_0, y_0) \in \mathbb{R}^{np} \times [-1, 1]^{np} \times \mathbb{R}^{np} \times \mathbb{R}^{mq} \times \mathbb{R}^{mq}$,

i): $V(x, z, y, \lambda, u)$ is positive definite, radically unbounded, and $V(x, z, y, \lambda, u) = 0$ holds if and only if $(x, z, y, \lambda, u) = (x^*, z^*, y^*, \lambda^*, u^*)$.

ii): The trajectories of $(x(t), z(t), y(t), \lambda(t), u(t))$ are bounded $\forall t \in [t_0, +\infty)$, or more precisely, $z(t) \in [-1, 1]^{np}$, and $(x^*, z^*, y^*, \lambda^*, u^*)$ of DCPNA-B (13) is Lyapunov stable.

iii): The trajectories of $(x(t), z(t), y(t), \lambda(t), u(t))$ are globally convergent and x(t) globally converges to a consensus optimal solution of the problem (11).

Proof:

For i): According to the definition of $V_0(x, z, y)$, $V_1(x)$ and $V_2(x)$, we have

$$V_{0}(\mathbf{x}, \mathbf{z}, \mathbf{y}) + V_{1}(\mathbf{x}) + V_{2}(\mathbf{z})$$

$$= h(\mathbf{x} + \mathbf{z}) - h(\mathbf{x}^{*} + \mathbf{z}^{*}) - (\mathbf{z} - \mathbf{z}^{*})^{T} \mathbf{z}^{*}$$

$$+ (\mathbf{A}\mathbf{x} - b - L_{c}\mathbf{y})^{T} \lambda^{*} - (\mathbf{x} - \mathbf{x}^{*})^{T} L_{r} \mathbf{u}^{*}$$

$$+ \frac{1}{2} \|\mathbf{x} - \mathbf{x}^{*}\|^{2} + \frac{1}{2} \|\mathbf{z} - \mathbf{z}^{*}\|^{2}$$

$$\geq (\mathbf{x} - \mathbf{x}^{*})^{T} (P_{[-1,1]^{np}}(\mathbf{x}^{*} + \mathbf{z}^{*}) + \mathbf{A}^{T} \lambda^{*} + L_{r} \mathbf{u}^{*})$$

$$= 0, \tag{20}$$

where the inequality holds from (20) and last equality is satisfied according to (17a). Thus, it is easy to obtain $V(x,z,y,\lambda,u)=0$ if $(x,z,y,\lambda,u)=(x^*,z^*,y^*,\lambda^*,u^*);$ $V(x,z,y,\lambda,u)>0$, otherwise, which means $V(x,z,y,\lambda,u)$ is positive definite. Moreover, we also obtain $V(x,z,y,\lambda,u)\to\infty$ as $\|(x,z,y,\lambda,u)\|\to\infty$, i.e., $V(x,z,y,\lambda,u)$ is radically unbounded.

For ii): The derivative of Lyapunov function $V(x, z, y, \lambda, u)$ along the trajectory of DCPNA-B (12) or (13) with Eq (17) satisfies

$$\dot{V}_{0}(x, z, y) = -\|P_{[-1,1]^{np}}(x+z) + A^{T}\lambda + L_{r}u\|^{2}
- (u - u^{*})^{T}L_{r}\dot{x} - (\lambda - \lambda^{*})^{T}A\dot{x}
- \frac{1}{2}(z^{*})^{T}(P_{[-1,1]^{np}}(x+z) - z)
+ \frac{1}{2}P_{[-1,1]^{np}}(x+z)^{T}(P_{[-1,1]^{np}}(x+z) - z), \quad (21)$$

$$\dot{V}_{1}(x) = (x - x^{*})^{T}\dot{x}
= (x - x^{*})^{T}L_{r}(u^{*} - u)$$

$$+ (\lambda^* - \lambda)^T A(x - x^*) + (x - x^*)^T$$

$$\times (P_{[-1,1]^{np}}(x^* + z^*) - P_{[-1,1]^{np}}(x + z)), \qquad (22)$$

$$\dot{V}_2(z) = (z - z^*)^T \dot{z}$$

$$= \frac{1}{2} (-z + P_{[-1,1]^{np}}(x + z))^T$$

$$\times (z - P_{[-1,1]^{np}}(x + z) + P_{[-1,1]^{np}}(x + z) - z^*)$$

$$= -\frac{1}{2} ||z - P_{[-1,1]^{np}}(x + z)||^2$$

$$- \frac{1}{2} (P_{[-1,1]^{np}}(x + z) - z^*)^T$$

$$\times (z - P_{[-1,1]^{np}}(x_{ij} + z_{ij})), \qquad (23)$$

$$\dot{V}_{3}(\mathbf{y}) = (\mathbf{y} - \mathbf{y}^{*})^{T} \dot{\mathbf{y}} = (\mathbf{y} - \mathbf{y}^{*})^{T} L_{c} \lambda, \tag{24}$$

$$\dot{V}_{4}(\lambda) = (\lambda - \lambda^{*})^{T} \dot{\lambda}$$

$$= (\lambda - \lambda^{*})^{T} (\mathbf{A}(\mathbf{x} + \dot{\mathbf{x}}) - b - L_{c}(\mathbf{y} + \lambda))$$

$$= (\lambda - \lambda^{*})^{T} \mathbf{A}(\mathbf{x} - \mathbf{x}^{*}) - \lambda^{T} L_{c} \lambda,$$

$$+ (\lambda - \lambda^{*})^{T} A \dot{\mathbf{x}} + \lambda^{T} L_{c} (\mathbf{y}^{*} - \mathbf{y}),$$
(25)

and

$$\dot{V}_{5}(\mathbf{u}) = (\mathbf{u} - \mathbf{u}^{*})^{T} \dot{\mathbf{u}}
= (\mathbf{u} - \mathbf{u}^{*})^{T} L_{r} \mathbf{x} + (\mathbf{u} - \mathbf{u}^{*})^{T} L_{r} \dot{\mathbf{x}}.$$
(26)

Combining with (21), (22), (23), (24), (25) and (26), one can obtain

$$\begin{split} \dot{V}(\mathbf{x}, \mathbf{z}, \mathbf{y}, \lambda, \mathbf{u}) &= - \left\| P_{[-1,1]^{np}}(\mathbf{x} + \mathbf{z}) + \mathbf{A}^{T} \lambda + L_{r} \mathbf{u} \right\|^{2} \\ &- \frac{1}{2} \left\| \mathbf{z} - P_{[-1,1]^{np}}(\mathbf{x} + \mathbf{z}) - \mathbf{z}^{*} \right\|^{2} \\ &+ \frac{1}{2} \left(P_{[-1,1]^{np}}(\mathbf{x} + \mathbf{z}) - \mathbf{z}^{*} \right)^{T} \\ &\times \left(P_{[-1,1]^{np}}(\mathbf{x} + \mathbf{z}) - \mathbf{z} \right) \\ &- \lambda^{T} L_{c} \lambda + \left(\mathbf{x} - \mathbf{x}^{*} \right)^{T} \\ &\times \left(\mathbf{z}^{*} - P_{[-1,1]^{np}}(\mathbf{x} + \mathbf{z}) \right) \\ &+ \frac{1}{2} \left(P_{[-1,1]^{np}}(\mathbf{x} + \mathbf{z}) - \mathbf{z}^{*} \right)^{T} \\ &\times \left(P_{[-1,1]^{np}}(\mathbf{x} + \mathbf{z}) - \mathbf{z} \right) \\ &= - \left\| P_{[-1,1]^{np}}(\mathbf{x} + \mathbf{z}) + \mathbf{A}^{T} \lambda + L_{r} \mathbf{u} \right\|^{2} \\ &- \frac{1}{2} \left\| \mathbf{z} - P_{[-1,1]^{np}}(\mathbf{x} + \mathbf{z}) \right\|^{2} - \lambda^{T} L_{c} \lambda \end{split}$$

$$+ (P_{[-1,1]^{np}}(x+z) - z^*)^T$$

$$\times (P_{[-1,1]^{np}}(x+z) - z - x + x^*)$$

$$\le - \|P_{[-1,1]^{np}}(x+z) + A^T \lambda + L_r u\|^2$$

$$- \frac{1}{2} \|z - P_{[-1,1]^{np}}(x+z)\|^2 - \lambda^T L_c \lambda$$

$$\le 0,$$

$$(27)$$

where the first inequality is satisfied by using the following projection inequality in Lemma 1

$$(P_{[-1,1]^{np}}(x+z) - z^*)^T (x+z - P_{[-1,1]^{np}}(x+z)) \ge 0,$$

and variational inequalities

$$(P_{[-1,1]^{np}}(x+z)-z^*)^T(-x^*) \ge 0.$$

The last inequality holds due to the semi-positive characterization of the matrix L_c and L_r .

From (27), one has $V(\mathbf{x}(t), \mathbf{z}(t), \mathbf{y}(t), \lambda(t), \mathbf{u}(t))$ $\leq V(x_0, z_0, y_0, \lambda_0, u_0) < +\infty$, which means the trajectories of $(x(t), z(t), y(t), \lambda(t), u(t))$ are bounded and $(x^*, z^*, y^*, \lambda^*, u^*)$ of DCPNA-B (13) is Lyapunov stable.

For the $\dot{z}(t) + \frac{1}{2}z(t) = \frac{1}{2}P_{[-1,1]^{np}}(x(t) + z(t))$ in DCPNA-B (13), by a simple integration procedure, we have

$$z(t) = e^{-\frac{t}{2}} z_0 + e^{-\frac{t}{2}} \int_{t_0}^t P_{[-1,1]^{np}}(x(s) + z(s)) e^{-\frac{s}{2}} ds,$$

which is equivalent to

$$z(t) = e^{-\frac{t}{2}} z_0$$

$$+ \left(1 - e^{-\frac{t}{2}}\right) \int_{t_0}^t \frac{e^{-\frac{s}{2}}}{e^{-\frac{t}{2}} - 1} P_{[-1,1]^{np}}(x(s) + z(s)) ds. \tag{28}$$

Since $\frac{e^{-\frac{s}{2}}}{e^{-\frac{t}{2}}-1} > 0$, $P_{[-1,1]^{np}}(\mathbf{x}(s)+\mathbf{z}(s)) \in [-1,1]^{np}$, $\forall t_0 \le s \le t$ and $[-1,1]^{np}$ is a closed and convex set, one has

$$\int_{t_0}^t \frac{e^{-\frac{s}{2}}}{e^{-\frac{t}{2}} - 1} P_{[-1,1]^{np}}(\mathbf{x}(s) + \mathbf{z}(s)) ds \in [-1,1]^{np}.$$

Since $z_0 \in [-1, 1]^{np}$, which means $z(t) \in [-1, 1]^{np}, \forall t \in$ $[t_0, +\infty).$

For iii): Define

$$R = \{(x, z, y, \lambda, u) : \dot{V}(x(t_T), z(t_T), y(t_T), \lambda(t_T), u(t_T)) = 0\}$$

$$\subseteq \{(x, z, y, \lambda, u) : \dot{x} = 0_{np}, \dot{z} = 0_{np}, \dot{y} = 0_{mq}\}. \quad (29)$$

Let M be the largest invariant set of R. According to the LaSalle's invariance principle of differential equation, $(x(t), z(t), y(t), \lambda(t), u(t)) \rightarrow M$ as $t \rightarrow \infty$. Assume $(\bar{\mathbf{x}}(t), \bar{\mathbf{z}}(t), \bar{\mathbf{y}}(t), \lambda(t), \bar{\mathbf{u}}(t))$ is a trajectory of DCPNA-B (13) with $(\bar{\mathbf{x}}(t_T), \bar{\mathbf{z}}(t_T), \bar{\mathbf{y}}(t_T), \bar{\lambda}(t_T), \bar{\mathbf{u}}(t_T)) \in \mathbf{M}$. Then, $(\bar{\mathbf{x}}(t), \bar{\mathbf{z}}(t), \bar{\mathbf{y}}(t), \bar{\lambda}(t), \bar{\mathbf{u}}(t)) \in \mathbf{M}, \ \forall \ t \geq t_{\mathrm{T}}.$ Therefore, for any $t \ge t_T$, $\dot{\mathbf{x}}(t) \equiv \mathbf{0}_{np}$, $\dot{\mathbf{z}}(t) \equiv \mathbf{0}_{np}$, $\dot{\mathbf{y}}(t) \equiv \mathbf{0}_{mq}$ and

$$\dot{\bar{\mathbf{u}}}(t) \equiv L_r \bar{\mathbf{x}}(t_{\mathrm{T}}) \equiv \mathcal{D},\tag{30a}$$

$$\dot{\bar{\lambda}}(t) \equiv A\bar{\mathbf{x}}(t_{\mathrm{T}}) - b - L_{c}(\mathbf{y}(t_{\mathrm{T}}) + \lambda(t_{\mathrm{T}})) \equiv \mathcal{C}. \tag{30b}$$

If $\mathcal{D} \neq 0_{np}$ and $\mathcal{C} \neq 0_{mq}$, then $\bar{\mathbf{u}}(t)$ and $\bar{\lambda}(t)$ are unbounded, which leads to a contradiction. Therefore,

$$M \subseteq \{(x, z, y, \lambda, u) : \dot{x} = 0_{np}, \dot{z} = 0_{np}, \dot{y} = 0_{mq}, \dot{\lambda} = 0_{mq}, \dot{u} = 0_{np}\},$$
(31)

the which implies following of trajectories $(x(t), z(t), y(t), \lambda(t), u(t))$ globally converge the equilibrium point of problem (11). From **Theorem 1**, we obtain that x(t) globally converges to a consensus optimal solution of the problem (11). Thus, the proof is completed.

V. NUMERICAL SIMULATIONS

In this section, numerical experiments on sparse signal and image recovery are performed to show the effectiveness of our proposed DCPNA-B (13), and the flowcharts of DCPNA-B (13) for sparse signal and image recovery are given in Fig. 4.

A. Sparse Signal Recovery

For DCPNA-B (13): Let measurement matrix be $A \in$ $\mathbb{R}^{50\times 100}$, and x be a real sparse signal with 10 sparsity, i.e., S = 10, which are randomly generalized. The observation vector b is obtained by Ax = b. Separating the matrix A into blocks with p = 5 and q = 4, that is, 5 by rows and 4 by columns. The communication graphs on \mathcal{G}^{row} and \mathcal{G}^{col} are given in Fig. 5 (top: left). Accordingly, the Laplacian

$$(t) = e^{-\frac{t}{2}} z_0 + e^{-\frac{t}{2}} \int_{t_0}^t P_{[-1,1]^{np}}(x(s) + z(s)) e^{-\frac{s}{2}} ds,$$
in is equivalent to
$$z(t) = e^{-\frac{t}{2}} z_0$$

$$+ \left(1 - e^{-\frac{t}{2}}\right) \int_{t_0}^t \frac{e^{-\frac{s}{2}}}{e^{-\frac{t}{2}} - 1} P_{[-1,1]^{np}}(x(s) + z(s)) ds. (28)$$

$$ce \frac{e^{-\frac{s}{2}}}{e^{-\frac{t}{2}} - 1} > 0, P_{[-1,1]^{np}}(x(s) + z(s)) \in [-1,1]^{np}, \forall t_0 \le 0$$
and $[-1,1]^{np}$ is a closed and convex set one has

sparse signal in a distributed manner.

The results of convergence and effectiveness of trajectories x(t) and $\lambda(t)$ of the DCPNA-B (13) are displayed in the bottom left and right subplots of Fig. 5, respectively. Fig. 5 (bottom: left) illustrates that the trajectory x(t) of the proposed DCPNA-B (13) is globally asymptotically stable, and their optimal solution is almost the same to the original sparse signal. As shown in Fig. 5 (bottom: left), it is observed that the $\lambda(t)$ of DCPNA-B (13) is globally and uniformly asymptotically stable as t increases.

B. Comparative Tests of Sparse Recovery

In addition, in order to show the superiority of DCPNA-B (13), we compare it with distributed continuous-time neurodynamic approaches including CNA-R [26], DCPNA-B [27] and TLDAN [28] in Fig. 6 (left) in the case of matrix A row partition with a communication graph on \mathcal{G}^{row} in Fig. 5 (top:left), and compare it to state-of-the-art distributed continuous-time neurodynamic approaches which contain CNA-C [26] and DCPNA-C [27] in Fig. 6 (right) with matrix A column partition and a communication graph on \mathcal{G}^{col} in Fig. 5 (top:left). As can be seen from Fig. 6 (left) that the DCPNA-B (13) with q = 1 has the fastest convergence rate because it contains two derivative feedback terms

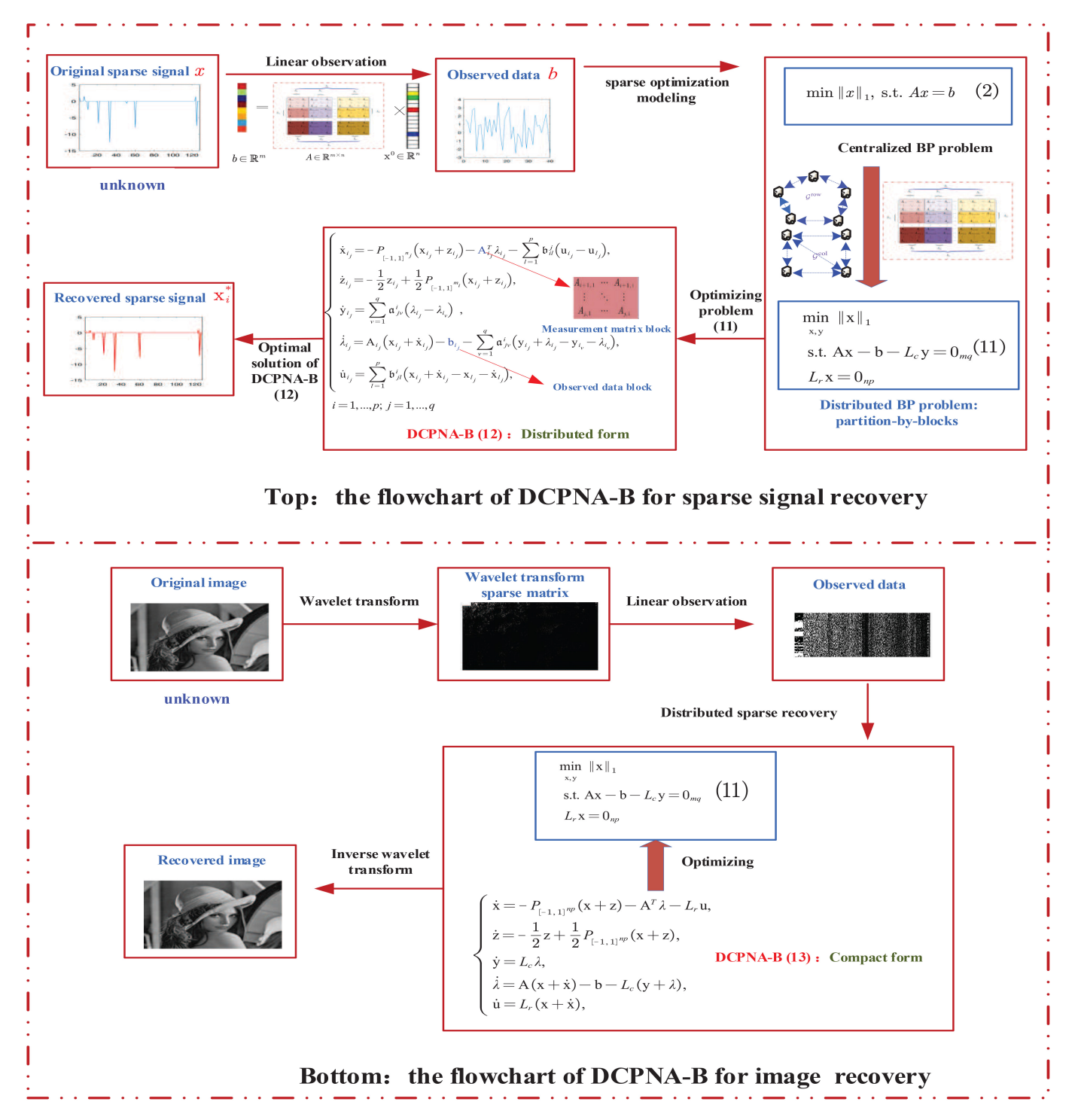


Fig. 4. The flowcharts of DCPNA-B (13) for sparse signal and image recovery.

and has more communication, moreover, DCPNA-B [27] and TLDAN [28] have faster convergence rate than CNA-R [26] due to they have less few projection calculations. It can be seen from Fig. 6 (right) that DCPNA-B (13) with p=1 provides a relatively faster convergence rate compared to CNA-C [26] and DCPNA-C [27].

To better demonstrate the superiority of the DCPNA-B (13), we compare DCPNA-B (13) with state-of-the-art neurodynamic approaches, including, distributed neurodynamic approaches: DCPNA-R [27], CNA-R [26], TLDAN [28],

DCPNA-C [27], CNA-C [26], centralized neurodynamic approaches: PNNSR [20] and LPNN-LCA [21]. The comparison results are shown in TABLE I.

In TABLE I, we gauge the performance of the neurodynamic approaches by the relative error (RelErr= $\frac{\|x^*-x^o\|}{\|x^o\|}$, where x^* is the recovered signal and x^o means original signal) between the reconstructed sparse signal and the original signal, where the bold values in each rank denote the best results on RelErr. From TABLE I, we can obtain that the proposed DCPNA-B (13) has the best performance at

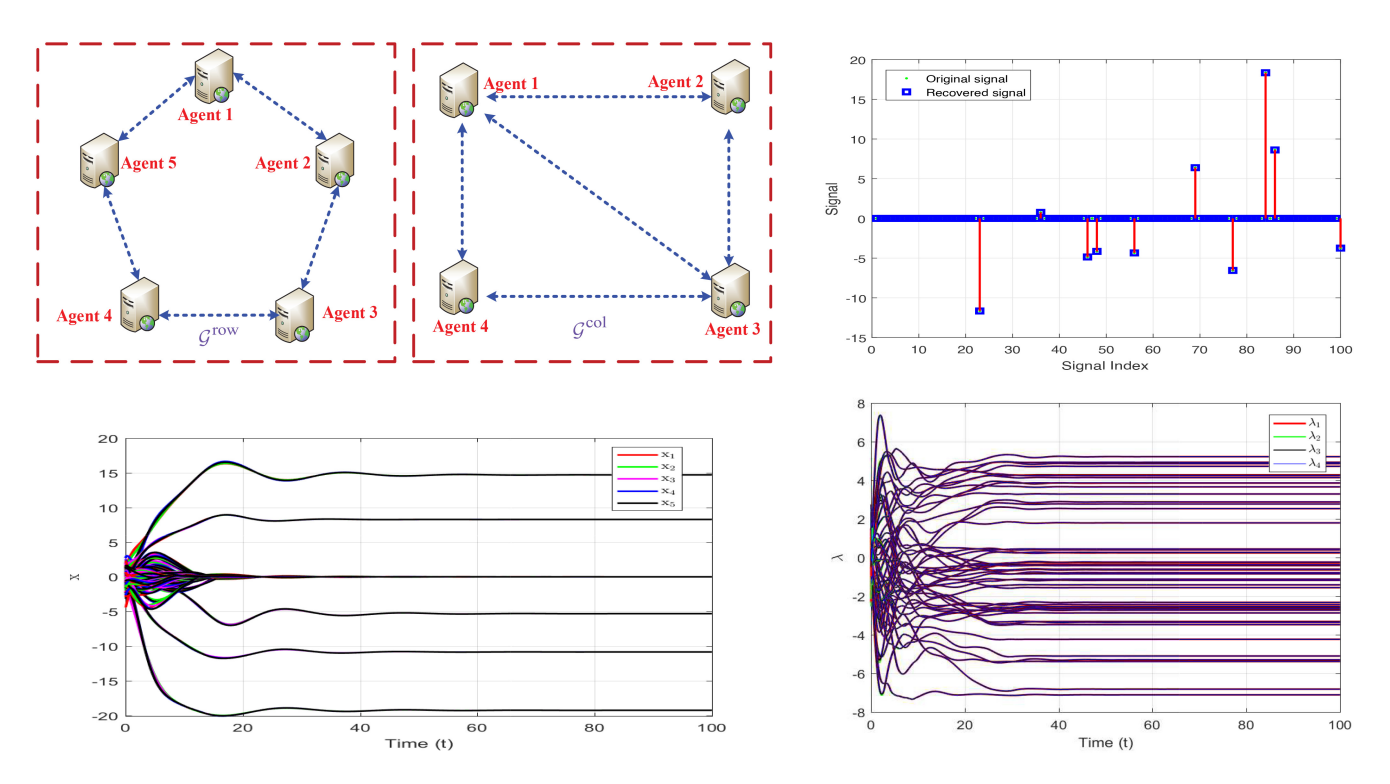


Fig. 5. (top: left) DCPNA-B (13) for problem (11) with p = 5 and q = 4. (top: right) Recovery performance of x. (bottom: left) States transition curves of x. (bottom: right) States transition curves of λ .

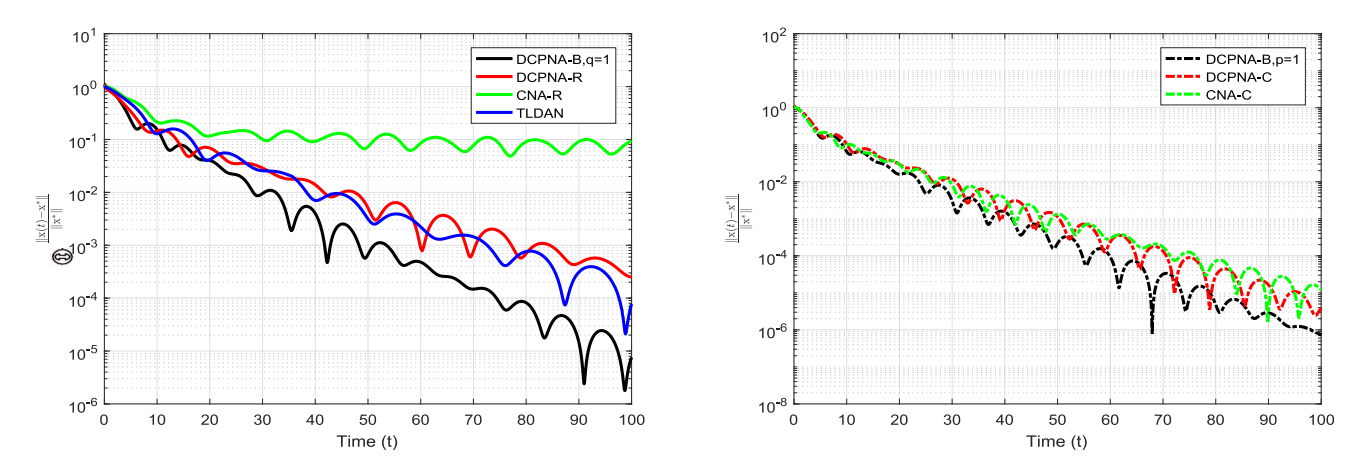


Fig. 6. Convergence rate for problem (11) with various distributed neurodynamic approaches. (left) Matrix A row partition; (right) Matrix A column partition.

TABLE I COMPARISON OF DCPNA-B (13), DCPNA-R [27], CNA-R [26], TLDAN [28], DCPNA-C [27], CNA-C [26], PNNSR [20] AND LPNN-LCA [21] When $m=\frac{n}{2}$ and $S=\frac{m}{8}$

Neurodynamic approaches	DCPNA-B (13)	DCPNA-R	CNA-R	TLDAN	DCPNA-C	CNA-C	LPNN-LCA	PNNSR
n	RelErr	RelErr	RelErr	RelErr	RelErr	RelErr	RelErr	RelErr
64	1.0582e-16	6.3515e-16	1.3748e-15	7.6011e-16	5.8112e-16	2.6518e-15	1.4505e-16	2.5868e-16
128	1.7372e-16	7.5788e-16	1.8745e-15	7.8416e-16	8.1349e-16	3.0072e-15	2.1297e-16	2.7813e-16
256	2.4696e-16	8.7278e-16	2.3561e-15	2.4756e-15	8.2724e-16	3.2724e-15	2.2096e-16	3.0061e-16
512	4.2037e-16	9.1268e-16	4.4214e-15	3.8451e-15	1.3152e-15	5.1863e-15	3.9547e-16	8.2562e-16
1024	4.6488e-16	9.2223e-15	3.7542e-14	5.2189e-15	2.5092e-15	8.7145e-14	4.8332e-16	3.2564e-15

n=64,128 and 1024. When n=256 and 512, the performance of LPNN-LCA [21] is best. The DCPNA-B (13) outperforms distributed neurodynamic approaches

DCPNA-R [27], TLDAN [28], CNA-C [26] and centralized neurodynamic approach PNNSR [20] because DCPNA-R [27], TLDAN [28], CNA-C [26] and PNNSR [20] contain



Fig. 7. **Image: Text**, m = 240. (a) Original image. (b) Recovered image of DCPNA-B (13). (c) Recovered image of DCPNA-R [27]. (d) Recovered image of PNNSR [20]. (e) Recovered image of OMP [14].



Fig. 8. **Image: Phantom**, m = 210. (a) Original image. (b) Recovered image of DCPNA-B (13). (c) Recovered image of DCPNA-R [27]. (d) Recovered image of PNNSR [20]. (e) Recovered image of OMP [14].



Fig. 9. **Image: X-ray**, m = 240. (a) Original image. (b) Recovered image of DCPNA-B (13). (c) Recovered image of DCPNA-R [27]. (d) Recovered image of PNNSR [20]. (e) Recovered image of OMP [14].

the projection matrix $A^T(AA^T)^{-1}A$ (contains the inverse of the matrix), which affects the accuracy of the recovered sparse signal.

C. Image Recovery

Image reconstruction has been widely used in the field of engineering and science. The Gaussian matrix $A \in \mathbb{R}^{150 \times 256}$ acts as measurement matrix, the communication graphs of \mathcal{G}^{row} and \mathcal{G}^{col} are shown in Fig. 5 (left) and the noise ratio (PSNR) is used to measure the quality of the reconstructed image, PSNR is given by

PSNR =
$$10 \log_{10} \frac{255^2}{\text{MSE}}$$
,

$$\text{MSE} = \frac{1}{n \times n} \sum_{i,j} (\hat{x}(i,j) - x(i,j))^2$$
,

where $\hat{x}(i,j)$, x(i,j) represent the pixels of the original image and the recovered image, respectively.

"In order to further verify the effectiveness of the proposed neurodynamic approach, we applied DCPNA-B (13) to the reconstruction of three different types of images, i.e., binary image ("Text" in Fig. 7 (a)), multivalue image ("Phantom" in Fig. 8 (a)) and natural image ("X-ray" in Fig. 9 (a)) but of the same size "256 \times 256". The restoration results for binary image ("Text") of a test when m = 240 in Fig. 7, the

recovered results of multivalue image ("Phantom") of a test when m=210 is displayed in Fig. 8 and the restored image results of natural image ("X-ray") of a test when m=240 is shown in Fig. 9. Moreover, the mean PSNR value of 20 times are displayed in TABLE II, which is used to measure the reconstructed effect of the proposed DCPNA-B (13). The results in TABLE II and Figs. 7–9 illustrate that the mean PSNR values of DCPNA-B (13) are the best compared to distributed neurodynamic approach: DCPNA-R [27], centralized neurodynamic approaches: PNNSR [20] and OMP [14], which is probably due to the fact that DCPNA-B (13) has no matrix inverse operation (there are round-off errors) and guarantees convergence to the global optimal solution based on optimization theory.

Remark 1: This paper focuses on distributed sparse theory and distributed approach that enable accurate reconstruction of sparse signals and images in noise-free condition, and provides theoretical and technical support for processing signals and images in mass-market consumer electronics (televisions, video recorders, VCRs, camcorders, radios, portable digital cameras, cameras on cell phones, etc.). We extend the theory of compressed sensing and provide new ideas for the development of single-pixel cameras based on the theory of compressed sensing (the core technology is sparse reconstruction problems and algorithms). For example, based on compressed sensing theory, the authors in [5] proposed

observed value: m	150 Mean PSNR	180 Mean PSNR	210 Mean PSNR	240 Mean PSNR						
	Micali I SINIX	Micali I SINK	Micali I SINIC	Wicali I SINK						
Image: Text										
DCPNA-B (13)	20.121	22.824	27.506	34.143						
DCPNA-R [27]	19.792	22.680	26.736	33.782						
PNNSR [20]	19.820	22.696	26.782	33.822						
OMP [14]	16.929	17.856	19.719	20.822						
Image: Phantom										
DCPNA-B (13)	38.895	44.750	51.745	65.451						
DCPNA-R [27]	38.675	44.015	51.728	65.051						
PNNSR [20]	38.642	44.322	51.757	64.404						
OMP [14]	33.925	37.745	40.512	43.036						
Image: X-ray										
DCPNA-B (13)	32.561	35.261	39.624	46.880						
DCPNA-R [27]	32.212	35.142	39.297	46.615						
PNNSR [20]	32.113	35.077	39.324	46.541						
OMP [14]	29.183	30.889	32.696	33.933						

TABLE II MEAN PSNR FOR THREE DIFFERENT TYPES OF IMAGES WITH DIFFERENT OBSERVED VALUE m

a low-complexity depth video codec to efficiently compress depth video; inspired by the sparse representability of high-resolution images, the authors in [30] proposed a sparse-based super-resolution method based on dictionary learning, it can address the issue of limited resolution in electronic imaging devices, where the sparse representation is associated with a sparse optimization problem, and the method they use involves sparse reconstruction.

Remark 2: According to the compressive sensing theory in [31], the sparse signal can be effectively reconstructed, the sampling value m needs to satisfy a certain condition, i.e., $m \ge C\delta^{-2} s \ln(\frac{eN}{s})$ in which C > 0 does not depend on s, m and N, e is the natural number, δ is depended on RIP condition. It is practically impossible to give the exact values of C > 0 and δ due to the complexity of their calculation. From $m \ge C\delta^{-2} s \ln(\frac{eN}{s})$, it is easy to see that the sampling value m is basically proportional to the sparsity s (where $\ln(\frac{eN}{s})$) has a very small effect compared to s), that is, when the sparsity s is fixed (in image reconstruction), the larger the sampling value m to satisfy the condition $m > C\delta^{-2} s \ln(\frac{eN}{s})$, the greater the probability to accurately reconstruct the sparse signal, to get better reconstruction performance (see TABLE II), we must choose suitable sampling value m. However, when the choice of m is small, that is, it does not satisfy the formula $m \ge C\delta^{-2} s \ln(\frac{eN}{s})$, the sparse signal can not be well reconstructed and therefore lead to worse image reconstruction results (see TABLE II).

VI. CONCLUSION

This paper has proposed a novel projection neurodynamic approach in continuous-time (named as DCPNA-B) for sparse recovery by solving BP problem with block partition of matrix A, which is a general model of BP with row partition and column partition of matrix A. First, a standard distributed BP problem based on the observation matrix block partition was obtained by using the distributed consensus

theory and supplement variables method. Then, a DCPNA-B was presented in the form of projection operator and the primal-dual dynamics, and the optimality and convergence of the DCPNA-B were also analyzed theoretically. Last, simulation results with sparse signal and image recovery have demonstrated the effectiveness and superiority of DCPNA-B. Considering that the communication topology between agents in practice is sometimes a directed graph, we plan to study distributed sparse signal reconstruction models and corresponding distributed neurodynamic approaches under directed communication topology in future work. Compared to Basis Pursuit problem (L_1 -norm model), nonconvex sparse signal models such as L_p , (1 > p > 0)-norm, L_{1-2} -hybrid norm models have the advantages of less sampling and promote sparsity. Therefore the distributed nonconvex sparse signal problems and the corresponding distributed neurodynamic approaches will be investigated in our future work. In addition, designing distributed neurodynamic approaches for solving sparse recovery problems that can denoise and apply them to multimedia sensing image reconstruction in consumer electronics will be part of our future research program.

REFERENCES

- [1] N.-I. Heo, D. S. Han, and H.-S. Oh, "Adaptive sparse equalizer robust to fast fading and long delay spread for ATSC DTV," *IEEE Trans. Consum. Electron.*, vol. 51, no. 3, pp. 803–808, Aug. 2005.
- [2] H.-S. Oh, D. S. Han, C. H. Lim, and D. J. Rhee, "Sparse equalizer using adaptive weight activation for fast start-up in ATSC DTV systems," *IEEE Trans. Consum. Electron.*, vol. 52, no. 1, pp. 92–96, Feb. 2006.
- [3] L. Zhang, J. Yang, K. Lu, and Q. Zhang, "Modified subspace method based on convex model for underdetermined blind speech separation," *IEEE Trans. Consum. Electron.*, vol. 60, no. 2, pp. 225–232, May 2014.
- [4] B. H. Tietche, O. Romain, and B. Denby, "Sparse channelizer for FPGA-based simultaneous multichannel DRM30 receiver," *IEEE Trans. Consum. Electron.*, vol. 61, no. 2, pp. 151–159, May 2015.
- [5] S. Wang, L. Yu, and S. Xiang, "A low complexity compressed sensing-based codec for consumer depth video sensors," *IEEE Trans. Consum. Electron.*, vol. 65, no. 4, pp. 434–443, Nov. 2019.
- [6] J. Wright, Y. Ma, J. Mairal, G. Sapiro, T. S. Huang, and S. Yan "Sparse representation for computer vision and pattern recognition," *Proc. IEEE*, vol. 98, no. 6, pp. 1031–1044, Jun. 2010.

- [7] F. Bach, J. Mairal, J. Ponce, and G. Sapiro, "Sparse coding and dictionary learning for image analysis," in *Proc. Int. Conf. Adv. Comput. Intell.*, 2010, pp. 1–52.
- [8] D. L. Donoho, "Compressed sensing," *IEEE Trans. Inf. Theory*, vol. 52, no. 4, pp. 1289–1306, Apr. 2006.
- [9] J. A. Tropp, "Just relax: Convex programming methods for identifying sparse signals," *IEEE Trans. Inf. Theory*, vol. 51, no. 3, pp. 1030–1051, Mar. 2006.
- [10] B. K. Natarajan, "Sparse approximate solutions to linear systems," SIAM J. Comput., vol. 24, no. 2, pp. 227–234, 1995.
- [11] E. J. Candés and T. Tao, "Decoding by linear programming," *IEEE Trans. Inf. Theory*, vol. 51, no. 12, pp. 4203–4215, Dec. 2005.
- [12] S. S. Chen, D. L. Donoho, and M. A. Saunders, "Atomic decomposition by basis pursuit," SIAM Rev., vol. 43, no. 1, pp. 129–159, 2001.
- [13] S. G. Mallat and Z. Zhang, "Matching pursuits with time-frequency dictionaries," *IEEE Trans. Signal Process.*, vol. 41, no. 12, pp. 3397–3415, Dec. 1993.
- [14] J. A. Tropp and A. C. Gilbert, "Signal recovery from random measurements via orthogonal matching pursuit," *IEEE Trans. Inf. Theory*, vol. 53, no. 12, pp. 4655–4666, Dec. 2007.
- [15] S. Boyd, N. Parikh, E. Chu, B. Peleato, and J. Eckstein, "Distributed optimization and statistical learning via the alternating method of multipliers," *Found. Trends Mach. Learn.*, vol. 3, no. 1, pp. 1–122, 2011.
- [16] Y. Wang, G. Zhou, L. Caccetta, and W. Liu, "An alternative Lagrange-dual based algorithm for sparse signal reconstruction," *IEEE Trans. Signal Process.*, vol. 59, no. 4, pp. 1895–1901, Apr. 2011.
- [17] M. A. T. Figueiredo, R. D. Nowak, and S. J. Wright, "Gradient projection for sparse reconstruction: Application to compressed sensing and other inverse problems," *IEEE J. Sel. Topics Signal Process.*, vol. 1, no. 4, pp. 586–597, Dec. 2007.
- [18] E. J. Cands and M. B. Wakin, "An introduction to compressive sampling," *IEEE Signal Process. Mag.*, vol. 25, no. 2, pp. 21–30, Mar. 2008.
- [19] A. Balavoine, C. J. Rozell, and J. Romberg, "Convergence speed of a dynamical system for sparse recovery," *IEEE Trans. Signal Process.*, vol. 61, no. 17, pp. 4259–4269, Sep. 2013.
- [20] Q. Liu and J. Wang, "L₁-minimization algorithms for sparse signal reconstruction based on a projection neural network," *IEEE Trans.* Neural Netw. Learn. Syst., vol. 27, no. 3, pp. 698–707, Mar. 2016.

- [21] R. Feng, C. Leung, A. G. Constantinides, and W.-J. Zeng, "Lagrange programming neural network for nondifferentiable optimization problems in sparse approximation," *IEEE Trans. Neural Netw. Learn. Syst.*, vol. 28, no. 10, pp. 2395–2407, Oct. 2017.
- [22] L. Yu, G. Zheng, and J.-P. Barbot, "Dynamical sparse recovery with finite-time convergence," *IEEE Trans. Signal Process.*, vol. 65, no. 23, pp. 6146–6157, Dec. 2017.
- [23] X. He, H. Wen, and T. Huang, "A fixed-time projection neural network for solving L₁-minimization problem," *IEEE Trans. Neural Netw. Learn. Syst.*, vol. 33, no. 12, pp. 7818–7828, Dec. 2022, doi: 10.1109/TNNLS.2021.3088535.
- [24] B. Gharesifard and J. Cortés, "Distributed continuous-time convex optimization on weight-balanced digraphs," *IEEE Trans. Autom. Control*, vol. 59, no. 3, pp. 781–786, Mar. 2014.
- [25] Q. Liu and J. Wang, "A second-order multi-agent network for bound-constrained distributed optimization," *IEEE Trans. Autom. Control.*, vol. 60, no. 12, pp. 3310–3315, Dec. 2015.
- [26] Y. Zhao, X. Liao, X. He, and R. Tang, "Centralized and collective neurodynamic optimization approaches for sparse signal reconstruction via L₁-minimization," *IEEE Trans. Neural Netw. Learn. Syst.*, vol. 33, no. 12, pp. 7488–7501, Dec. 2022, doi: 10.1109/TNNLS.2021.3085314.
- [27] Y. Zhao, X. Liao, and X. He, "Distributed continuous and discrete time projection neurodynamic approaches for sparse recovery," *IEEE Trans. Emerg. Topics Comput. Intell.*, vol. 6, no. 6, pp. 1411–1426, Dec. 2022, doi: 10.1109/TETCI.2022.3170514.
- [28] J. Xu, X. He, X. Han, and H. Wen, "A two-layer distributed algorithm using neurodynamic system for solving L1-minimization," *IEEE Trans. Circuits Syst. II, Exp. Briefs*, vol. 69, no. 8, pp. 3490–3494, Aug. 2022.
- [29] M. F. Duarte et al., "Single-pixel imaging via compressive sampling," IEEE Signal Process. Mag., vol. 25, no. 2, pp. 83–91, Mar. 2008.
- [30] F. Zhou, W. Yang, and Q. Liao, "Single image super-resolution using incoherent sub-dictionaries learning," *IEEE Trans. Consum. Electron.*, vol. 58, no. 3, pp. 891–897, Aug. 2012.
- [31] R. G. Baraniuk, M. A. Davenport, R. A. DeVore, and M. Wakin, "A simple proof of the restricted isometry property for random matrices," *Construct. Approx.*, vol. 28, no. 3, pp. 253–263, 2008.